GMR
The Original

STRUCTURAL AND MORPHOLOGICAL CHARACTERIZATION OF ZINC NANOPARTICLES SYNTHESIZED USING *URGINEA INDICA* KUNTH (WILD ONION) EXTRACT

Apurwa Singh[1], Sanyogita Shahi[2]*
[1]Research Scholar, Department of Chemistry, Kalinga University, Raipur, Chhattisgarh 492101, India
[2]Professor, Department of Science (Chemistry), Kalinga University, Raipur, Chhattisgarh, 492101, India
*Corresponding Author: drsanyogitashahi@gmail.com

ABSTRACT
This study demonstrates a green, plant-mediated synthesis protocol for zinc nanoparticles (ZnNPs) using a hydroethanolic bulb extract of *Urginea indica* Kunth (Wild Onion) as a biogenic template for metal ion reduction and capping. Liquid Chromatography-Mass Spectrometry (LC-MS) characterization of the extract revealed a diverse spectrum of bio-functional secondary metabolites—including phenolics, flavonoids, and glycosidic derivatives—acting as key reducing and surface-passivating agents. Optical verification via Ultraviolet-Visible (UV-Vis) spectroscopy exhibited a prominent absorption maximum at 288–290 nm, confirming the biogenic nucleation of zinc-based nanostructures. X-ray Diffraction (XRD) analysis verified the polycrystalline phase structure of the ZnNPs with dominant reflection orientation at $2\theta = 32.5^0$. Scanning Electron Microscopy (SEM) and Transmission Electron Microscopy (TEM) revealed predominantly spherical to quasi-spherical nanoparticles forming porous, high-surface-area aggregates, with individual particle widths measuring 0.28–0.30 nm. Energy-Dispersive X-ray Spectroscopy (EDX) and elemental mapping confirmed high elemental purity, with zinc comprising 77.3 wt% alongside trace plant-derived nitrogen, sulfur, magnesium, and copper. This bio-template method provides an eco-friendly and scalable platform for synthesizing functional zinc nanomaterials, offering substantial utility for future downstream molecular applications, including bio-imaging, antimicrobial resistance mitigation, targeted drug delivery, and agricultural genetic enhancements.

KEYWORDS: *Urginea indica* Kunth; Green synthesis; Zinc nanoparticles; LC-MS profiling; Nanomaterial characterization; Bio-template platform

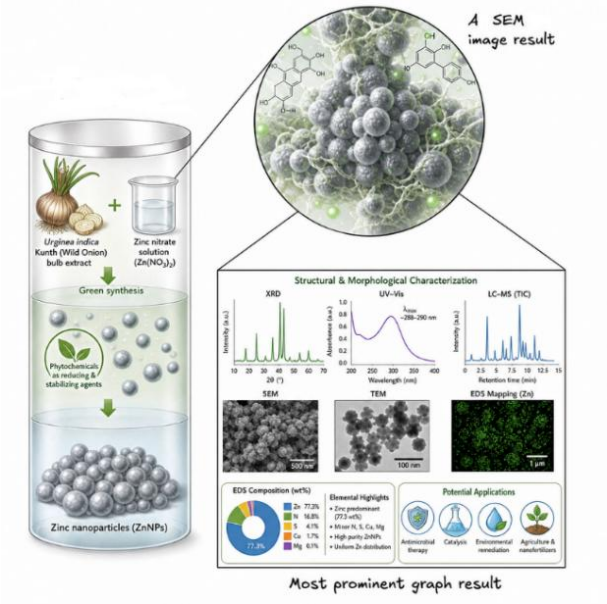

1. INTRODUCTION

Green nanotechnology and plant-mediated biogenic synthesis offer a sustainable, eco-friendly, and cost-effective alternative to conventional physical and chemical methods for nanoparticle production. Conventional physical

and chemical reduction strategies frequently rely on hazardous organic solvents, toxic reducing agents, and energy-intensive conditions, generating toxic byproducts and posing ecological risks. Biogenic approaches leverage plant secondary metabolites as natural reducing, capping, and stabilizing agents, facilitating one-pot nanoparticle formation under ambient temperatures and aqueous conditions. Zinc-based nanomaterials (ZnNPs and ZnO) possess unique physicochemical, optical, catalytic, and electronic properties, rendering them key candidates for diverse biotechnological, environmental, and agricultural applications. The mechanistic basis of plant-mediated synthesis involves three key phases:

(i) **Reduction:** Metal ions (Zn^{+2}) are reduced via electron transfer or complexation with redox-active phytochemicals.

(ii) **Nucleation and Growth:** Unstable zero-valent zinc atoms aggregate into nanoscale nuclei and grow into discrete nanoparticles.

(iii) **Stabilization:** Surface passivation by plant polysaccharides, proteins, and polyphenols limits over-aggregation and regulates final morphology.

Urginea indica Kunth (Wild Onion), a medicinal plant rich in bio-functional phytochemicals, contains bioactive secondary metabolites including cardiac glycosides, flavonoids, phenolics, saponins, and polysaccharides. These phytochemicals serve as natural electron donors and capping ligands. Although *U. indica* extracts have been documented for traditional pharmacological uses, their utility as a biogenic platform for zinc nanoparticle synthesis has remained systematically under-explored. Previous plant-mediated ZnNP studies often lack integrated structural and morphological characterization using combined LC-MS, high-resolution electron microscopy (SEM/TEM), and EDX elemental mapping. This study demonstrates a green synthesis route using a hydroethanolic extract of the bulb of *Urginea indica* Kunth. We report the structural, morphological, and chemical properties of the synthesized ZnNPs through UV-Vis spectroscopy, X-ray diffraction (XRD), SEM-EDX, TEM with line intensity profiling, and LC-MS phytochemical profiling.

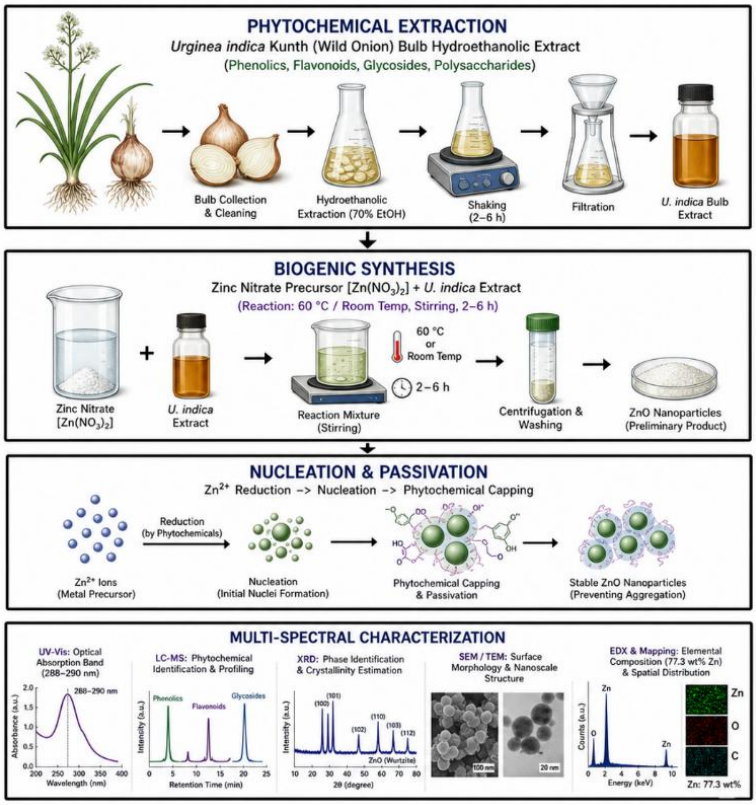

Figure 1. Operational workflow schematic for the biogenic synthesis and multi-spectral characterization of zinc nanoparticles using *Urginea indica* Kunth bulb extract.

2. LITERATURE REVIEW

2.1. Green Nanotechnology vs. Physical/Chemical Synthesis Routes

Chemical reduction (e.g., sodium borohydride, hydrazine hydrate) and physical techniques (e.g., laser ablation, thermal evaporation) yield uniform nanoparticle distributions but present operational drawbacks, including high energy requirements, hazardous waste production, and surface toxicity. Biogenic green synthesis operates under aqueous, low-toxicity, and low-energy conditions [Table 1]. Plant extracts offer operational advantages over microbial cultures (bacterial/fungal) by eliminating cell-culture maintenance, multi-step purification, and pathogenicity risks.

Table 1. Structural, Methodological, and Application Comparisons of Phytochemical-Mediated Zinc Nanoparticles.

Plant Bio-Template	Extract Medium	Dominant Nanoparticle Morphology	Particle Size Range / Features	Primary Characterization Methods	Functional Applications
Aloe barbadensis Miller	Aqueous	Hexagonal/ Spherical	25 – 55 nm	XRD, SEM, UV-Vis	Antibacterial, Optical
Citrus aurantifolia	Aqueous	Quasi-spherical	30 – 100 nm	XRD, TEM, FTIR	Catalytic, Antibacterial
Azadirachta indica	Aqueous	Spherical to Oval	18 – 35 nm	XRD, SEM, EDX	Antimicrobial, Agricultural
Camellia sinensis	Aqueous/ Ethanolic	Spherical	16 – 30 nm	UV-Vis, XRD, TEM	Photocatalytic, Antioxidant
Deverra tortuosa	Aqueous	Spherical	12 – 28 nm	XRD, TEM, Cytotoxicity	Cytotoxic/ Biomedical
Ocimum tenuiflorum	Hydroalcoholic	Hexagonal Wurtzite	20 – 45 nm	XRD, SEM, FTIR	Fungicidal, Agricultural
Allium cepa L. (Peel)	Aqueous Waste	Spherical/ Agglomerated	15 – 40 nm	UV-Vis, XRD, TEM, EDX	Antioxidant, Antibacterial
Urginea indica Kunth	Hydroethanolic	Quasi-Spherical/ Porous Aggregates	Nanoscale (~0.28-0.30 nm features)	LC-MS, UV-Vis, XRD, SEM-EDX, TEM	Biomedical, Catalytic, Agriculture

2.2. Phytochemical Drivers in *Urginea indica* Kunth

Urginea indica Kunth contains bio-functional secondary metabolites, such as bufadienolides, cardiac glycosides, quercetin derivatives, and phenolic acids [Figure 2].

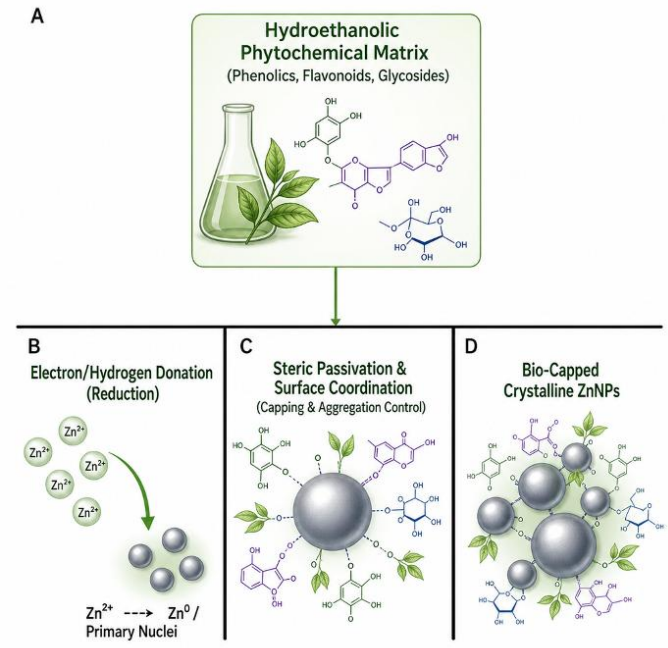

Figure 2. Proposed biogenic reduction and stabilization mechanism of Zn^{+2} into crystalline ZnNPs governed by *Urginea indica* phytochemicals.

The hydroxyl (-OH) and carbonyl (C=O) functional groups within phenolics and flavonoids donate electrons to reduce precursor zinc ions (Zn^{+2}) to zero-valent zinc (Zn^{0}) or zinc oxide coordination complexes. Simultaneously, macromolecular proteins and polysaccharides adsorb onto the growing nanoparticle facets via electrostatic interaction and steric hindrance, capping the surface and limiting uncontrolled growth.

2.3. Structural, Optical, and Morphological Analytical Frameworks

Comprehensive characterization of biogenic zinc nanoparticles requires a multi-technique approach:

2.3.1. **UV-Visible Spectroscopy:** Identifies the electronic transitions and characteristic optical absorption bands.
2.3.2. **X-Ray Diffraction (XRD):** Determines crystallographic structure, phase purity, and crystal size using the Debye-Scherrer equation:

$$D = \frac{K \cdot \lambda}{\beta \cdot \cos\theta}$$

Where: D = Crystallite size
K = Shape factor (~0.9)
λ = X-ray wavelength
β = Full Width at Half Maximum (FWHM)
θ = Bragg angle

2.3.3. **Electron Microscopy (SEM & TEM) and EDX:** Resolves surface topography, internal core size, spatial aggregation, elemental stoichiometry, and surface-bound impurities.
2.3.4. **Liquid Chromatography-Mass Spectrometry (LC-MS):** Profiles the specific secondary metabolite fractions in the plant extract, identifying the capping agents involved in biogenic stabilization.

3. MATERIALS AND METHODS

3.1. Collection and Preparation of Plant Material

Fresh bulbs of *Urginea indica* Kunth (Wild Onion) were procured from the local market in Raipur, Chhattisgarh, India. The bulbs were thoroughly washed under running tap water followed by rinsing with distilled water to remove adhering soil, dust, and other extraneous impurities. Cleaned bulbs were then cut into small pieces and manually crushed using a mortar and pestle to obtain a coarse paste, which served as the starting material for extract preparation.

3.2. Preparation of Plant Extract

The crushed plant material was subjected to maceration in a hydroethanolic solvent system consisting of ethanol and distilled water in 7:3 (v/v) ratio. The mixture was transferred to a closed container and kept at room temperature for 15–20 days, with intermittent stirring to enhance the diffusion and extraction of bioactive phytochemicals. After maceration, the mixture was further processed using Soxhlet extraction to achieve maximum recovery of phytoconstituents from the plant matrix. The combined extract was concentrated by evaporating the solvent under reduced pressure using a rotary evaporator until a viscous hydroethanolic extract was obtained. The concentrated extract was transferred to an airtight container and stored at 4 °C until use in nanoparticle synthesis and phytochemical analysis.

3.3. Green Synthesis of Zinc Nanoparticles

Green synthesis of zinc nanoparticles was carried out using the concentrated *Urginea indica* extract as a natural reducing and stabilizing agent. An aqueous solution of zinc nitrate, $Zn(NO_3)_2$, was prepared at a concentration of 0.1 M to serve as the metal precursor. Five millilitres (5 mL) of the plant extract was added dropwise to the zinc nitrate solution under continuous magnetic stirring to ensure homogeneous mixing and controlled reaction conditions. The reaction mixture was stirred for 6 hours at room temperature to facilitate the reduction of zinc ions and the subsequent nucleation and growth of zinc nanoparticles. A gradual change in the colour and appearance of the solution was observed, indicating the formation of nanoparticles. Upon completion of the reaction period, the suspension was filtered through Whatman No. 1 filter paper to remove unreacted plant residues and coarse particulates, yielding a colloidal dispersion of the synthesized zinc nanoparticles.

4. RESULT AND DISCUSSION

4.1. UV-Vis Spectroscopic Analysis

The UV–Visible absorption spectrum of the zinc nanoparticles synthesized using the hydroethanolic extract of *Urginea indica* Kunth demonstrates the successful formation of zinc-based nanoparticles.

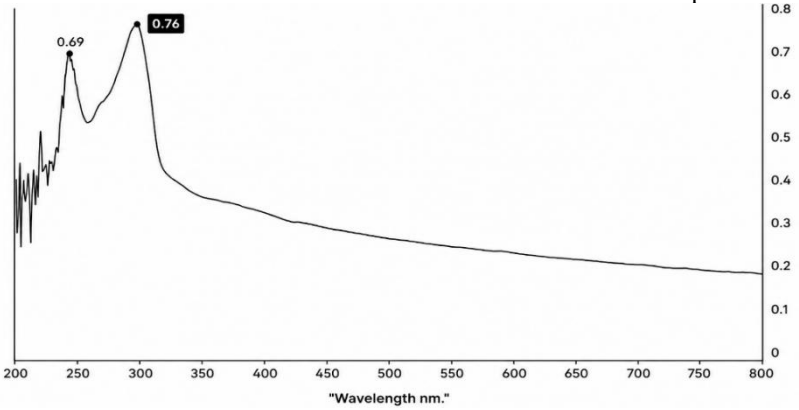

Figure 3: UV–Visible absorption spectrum of zinc nanoparticles synthesized using the hydroethanolic extract of *Urginea indica* Kunth (Wild Onion)

The spectrum exhibits two prominent absorption peaks, with the first peak observed at approximately 240 nm (absorbance ≈ 0.69) and the second, more intense peak at approximately 288–290 nm (absorbance ≈ 0.76). The stronger absorption peak around 290 nm represents the maximum absorbance (λ_{max}) and confirms the optical response associated with the formation of zinc nanoparticles. This absorption originates from the electronic transition of zinc oxide nanoparticles and is consistent with the characteristic UV absorption reported for bio-synthesized ZnO nanoparticles [Figure 3].

4.2. XRD Analysis

The X-ray diffraction (XRD) pattern illustrates the crystalline characteristics of the biosynthesized zinc nanoparticles. The diffraction profile exhibits several well-defined peaks over the 2θ range of 10°–70°, confirming the presence of crystalline phases within the synthesized sample. The most intense diffraction peak appears at approximately 32.5°, indicating the dominant crystalline orientation of the nanoparticles. Additional diffraction peaks are observed near 11.8°, 25°, 28°, 31°, 37–39°, 43–49°, 55–60°, and 61–69°, demonstrating the polycrystalline nature of the material. The indexed reflections correspond to Chlorite (002), Quartz (SiO_2) (100), and Calcite ($CaCO_3$) (104), as indicated by the reference lines in the diffractogram. The diffraction peaks labelled 002, 003, 004, 005, 006, 007, 008, together with crystallographic planes such as 100, 101, 102, 104, 110, 111, 113, 116, 122, 200, 201, 202, 203, 211, 214, and 220, confirm the presence of multiple crystalline domains. The sharpness and high intensity of the principal peaks indicate good crystallinity, whereas the broad background between 30° and 45° suggests the coexistence of a small amorphous fraction originating from phytochemicals adsorbed on the nanoparticle surface during green synthesis. The occurrence of minor mineral phases such as quartz and calcite may arise from naturally occurring inorganic constituents present in the *Urginea indica* extract or residual plant-derived minerals that remain associated with the nanoparticle surface. These phytochemical and mineral residues act as natural capping and stabilizing agents, preventing excessive particle growth and agglomeration [Figure 4].

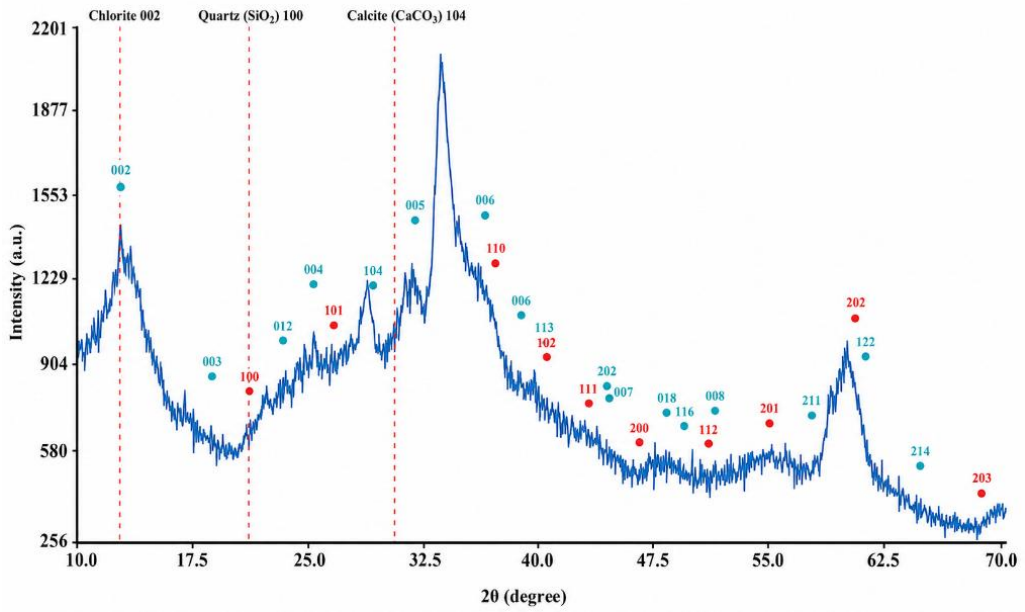

Figure 4: X-ray Diffraction (XRD) Pattern of Bio-synthesized Zinc Nanoparticles with Indexed Diffraction Peaks

4.3. SEM Analysis

The morphology of zinc nanoparticles (ZnNPs) synthesised using *Urginea indica* Kunth extract was examined through Scanning Electron Microscopy (SEM). Low-magnification SEM images [Figure 5] showed irregularly shaped clusters of highly agglomerated nanoparticles with rough, porous surfaces, typical in plant-mediated synthesis due to high surface energy and phytochemical interactions. Higher magnification [Figure 6] revealed predominantly spherical to quasi-spherical nanoparticles, densely packed and interconnected, suggesting effective nucleation and growth. The rough texture indicates that phytochemicals in the extract acted as reducing and stabilising agents, facilitating nanoparticle formation and controlling growth.

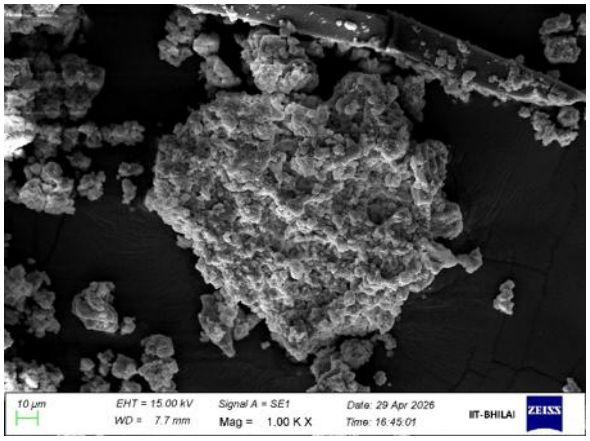

Figure 5: SEM image of green-synthesised ZnNPs synthesised using *Urginea indica* Kunth extract (1.00 KX).

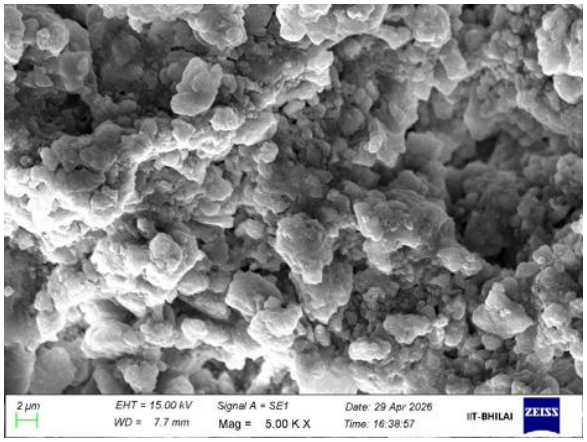

Figure 6: High-resolution SEM image of green-synthesised ZnNPs synthesised using *Urginea indica* Kunth extract (5.00 KX).

4.4. TEM Analysis

TEM micrographs recorded at 200-100 nm scale bars revealed that the nanoparticles were predominantly quasi-spherical to irregular in shape and formed densely aggregated clusters on the carbon-coated TEM grid. The lower-magnification image illustrated the overall distribution and aggregation of nanoparticles (Figure 7], whereas the higher-magnification image clearly distinguished individual particles with a heterogeneous size distribution and relatively rough surfaces [Figure 8]. The observed aggregation is attributed to phytochemicals present in the plant extract, which act as natural reducing, capping, and stabilizing agents during biosynthesis. Darker regions correspond to electron-dense nanoparticle aggregates, while lighter regions represent the supporting carbon film. No significant impurities or elongated nanostructures were observed, indicating the formation of relatively pure zinc nanoparticles. These nanoscale characteristics provide a high surface area suitable for biomedical, catalytic, environmental, and agricultural applications.

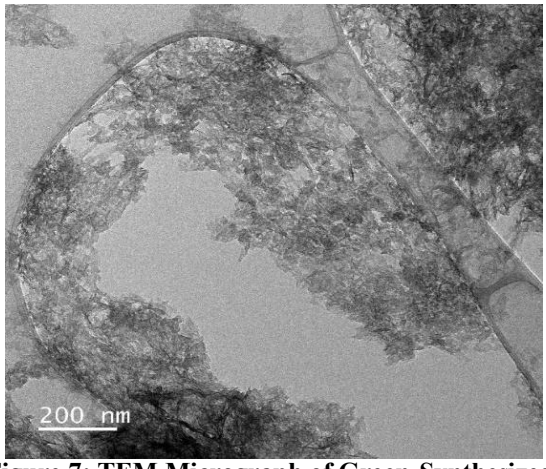

Figure 7: TEM Micrograph of Green-Synthesized Zinc Nanoparticles Using *Urginea indica* Kunth Extract in 200nm

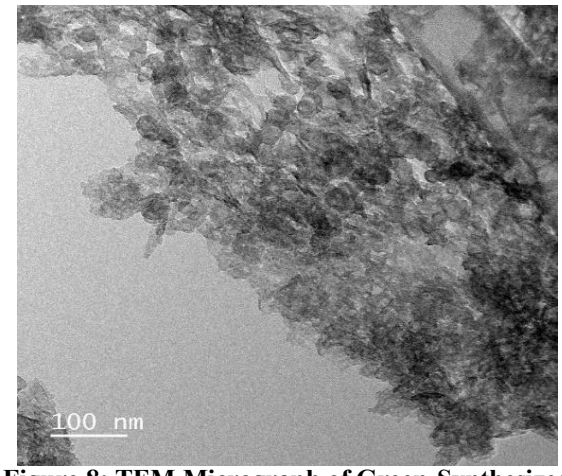

Figure 8: TEM Micrograph of Green-Synthesized Zinc Nanoparticles Using *Urginea indica* Kunth Extract in 100nm

The TEM line intensity profile provides quantitative information regarding the distribution and dimensions of the bio-synthesized zinc nanoparticles [Figure 9]. The profile exhibits a series of alternating peaks and valleys corresponding to variations in electron density across the selected measurement line. High-intensity peaks represent electron-dense zinc nanoparticle regions, whereas lower-intensity regions correspond to the carbon support film or spaces between adjacent nanoparticles. The presence of multiple peaks throughout the profile indicates that the nanoparticles are distributed as aggregated clusters rather than isolated particles, which is consistent with the TEM observations. The marked measurement region indicates a particle width of approximately 0.28–0.30 nm, demonstrating nanoscale particle dimensions. The fluctuations in intensity further suggest heterogeneity in particle size and aggregation, reflecting simultaneous nucleation and growth during the green synthesis process

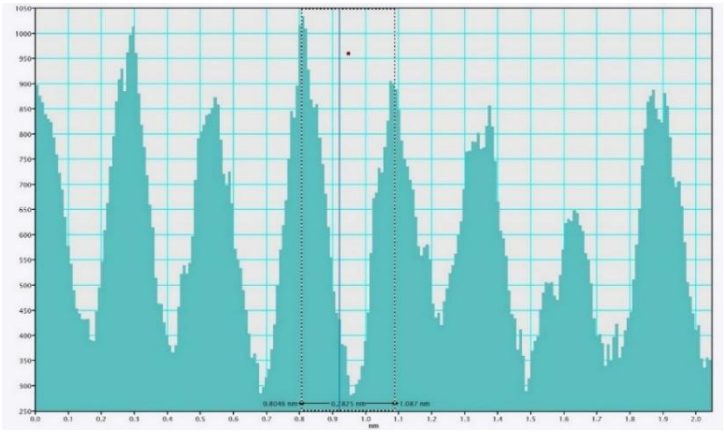

Figure 9: TEM Line Intensity Profile of Green-Synthesized Zinc Nanoparticles Using *Urginea indica* Kunth Extract

4.5. EDS Analysis

Energy-Dispersive X-ray Spectroscopy (EDX) analysed the elemental composition of green-synthesised zinc nanoparticles (ZnNPs) from *Urginea indica* extract. The EDX spectrum confirmed the predominant presence of zinc with peaks at 1.0 keV (Zn Lα) and 8.6 keV (Zn Kα), indicating a composition of 77.3 wt% zinc. Minor elements detected included nitrogen (16.8 wt%), sulfur (4.1 wt%), magnesium (0.1 wt%), and copper (1.7 wt%), suggesting residuals from the plant material and synthesis process. The low level of foreign elements indicates high purity of the nanoparticles, consistent with SEM observations and affirming the effectiveness of phytochemicals in reducing and stabilising zinc ions during synthesis [Figure 10].

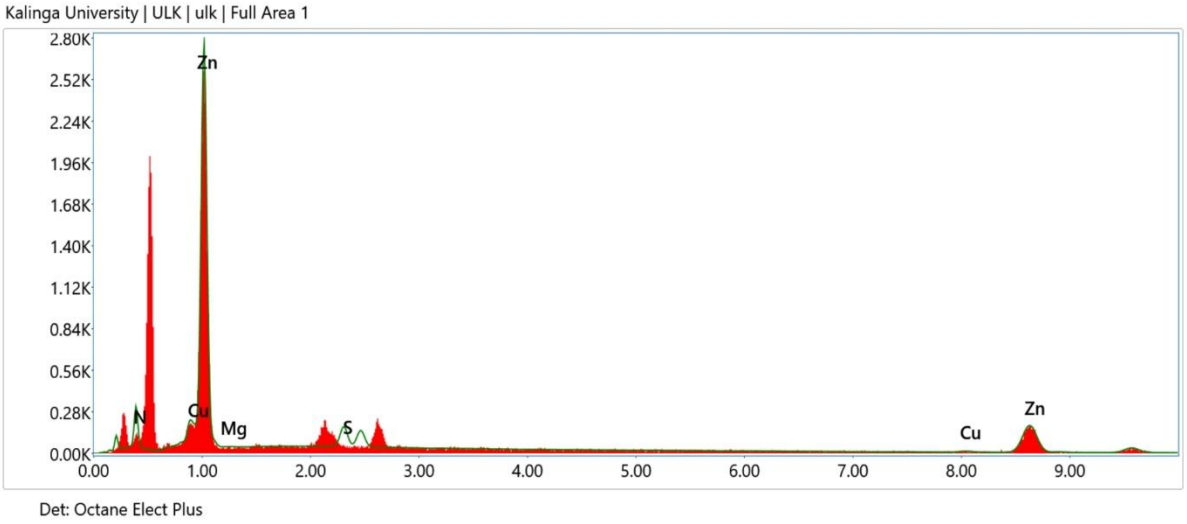

Figure 10: Energy-Dispersive X-ray Spectroscopy (EDX) spectrum of green-synthesised zinc nanoparticles synthesised using *Urginea indica* Kunth (Wild Onion) extract

The quantitative EDX analysis of green-synthesised zinc nanoparticles from *Urginea indica* Kunth extract reveals that zinc (Zn) is the primary element, comprising 77.3 wt% and 46.6 at%, validating the effective reduction of zinc ions. Nitrogen (N) and sulfur (S) are also present at 16.8 wt% and 4.1 wt%, respectively, likely from residual nitrate ions and sulfur-containing biomolecules in the extract. Trace amounts of copper (Cu) and magnesium (Mg) were detected, with zinc displaying the highest net intensity (98.0) and lowest error (6.5%), indicating reliable quantification. The reported correction factors are close to unity, ensuring the accuracy of the results and confirming the successful synthesis of zinc nanoparticles using *Urginea indica* extract [Table 2].

Table 2: Quantitative elemental composition of green-synthesised zinc nanoparticles synthesised using *Urginea indica* Kunth (Wild Onion) extract by Energy-Dispersive X-ray Spectroscopy (EDX).

Element	Weight %	MDL	Atomic %	Net Int.	Error %	R	A	F
N K	16.8	14.15	47.2	38.1	14.7	0.8118	0.1059	1.0000
Mg K	0.1	11.75	0.1	0.4	89.4	0.8452	0.1925	1.0022

S K	4.1	8.55	5.0	37.6	10.0	0.8686	0.6278	1.0108
Cu K	1.7	76.81	1.1	3.5	61.6	0.9491	0.9867	1.2341
Zn K	77.3	129.03	46.6	98.0	6.5	0.9574	0.9896	1.0467

4.6. Mapping Analysis

Elemental mapping using Energy-Dispersive X-ray Spectroscopy (EDS) analysed the spatial distribution of elements in green-synthesised zinc nanoparticles (ZnNPs) made from *Urginea indica* extract. The mapping revealed a uniform distribution of zinc (Zn), confirming effective reduction by phytochemicals from the extract. Minor signals for nitrogen (N), magnesium (Mg), sulfur (S), and copper (Cu) were detected but in lower intensities, indicating their sparse presence. The elemental analysis identified zinc as the predominant element at 77.3 wt%, demonstrating high elemental purity and successful green synthesis of ZnNPs. These results align with SEM findings, validating the synthesis method for structural and functional applications [Figure 11].

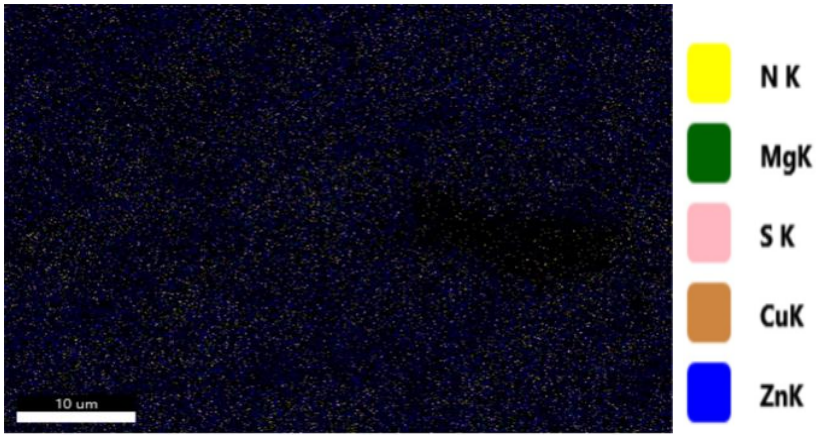

Figure 11: EDS elemental mapping of green-synthesised zinc nanoparticles using *Urginea indica* Kunth (Wild Onion) extract

4.7. Liquid Chromatography–Mass Spectrometry (LC–MS) Analysis

The LC–MS extracted ion chromatograms (EICs) of the hydroethanolic extract of *Urginea indica* Kunth revealed a diverse phytochemical profile represented by several molecular formulas, confirming the chemical complexity of the extract [Figure 12]. The EIC corresponding to $C_6H_6O_3$ exhibited a distinct chromatographic profile with a dominant peak at 8.094 min and additional peaks at 8.464, 8.850, and 9.371 min, indicating the presence of a major phytochemical together with structurally related compounds, isomers, or fragmentation products.

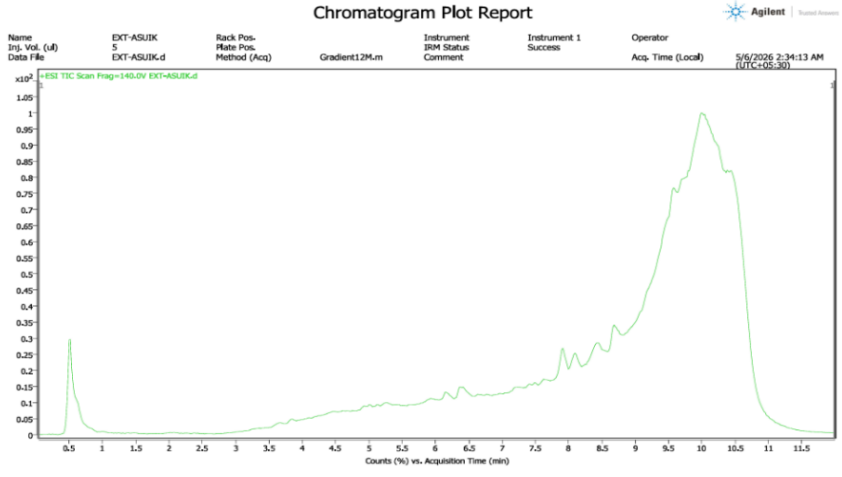

Figure 12: Total Ion Chromatogram (TIC) of the Hydroethanolic Extract of *Urginea indica* Kunth

The chromatographic signal was concentrated between 8.0 and 9.5 min, suggesting moderate retention characteristics and effective chromatographic separation [Figure 13a]. Similarly, the EIC of $C_{15}H_{22}O$ displayed two major peaks at 0.536 min and 4.298 min, indicating the presence of two compounds with the same molecular formula but different chromatographic behaviours, likely due to structural variations or isomerism. Additional low-intensity peaks observed between 1.5 and 5.5 min further indicated the occurrence of trace constituents,

whereas minimal chromatographic activity beyond 6.0 min suggested complete elution of the selected ion [Figure 13b].

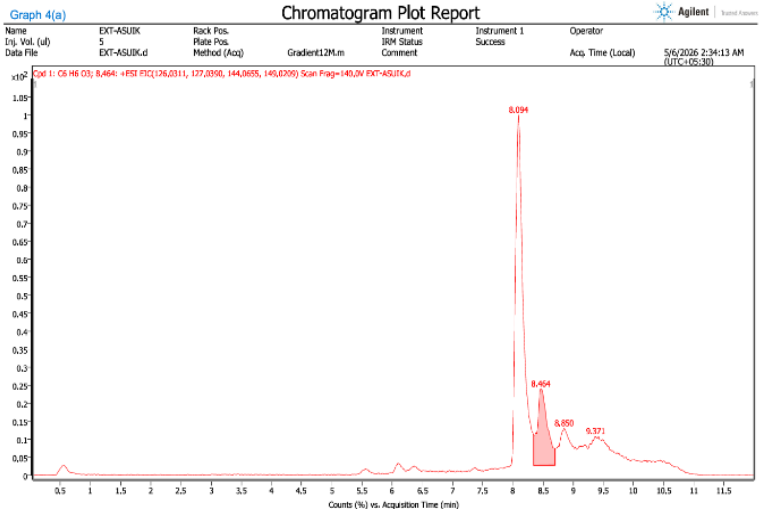

Figure 13 a : LC–MS chromatographic profile of the hydroethanolic extract of *Urginea indica* Kunth indicating the retention times of the detected $C_6H_6O_3$ compound.

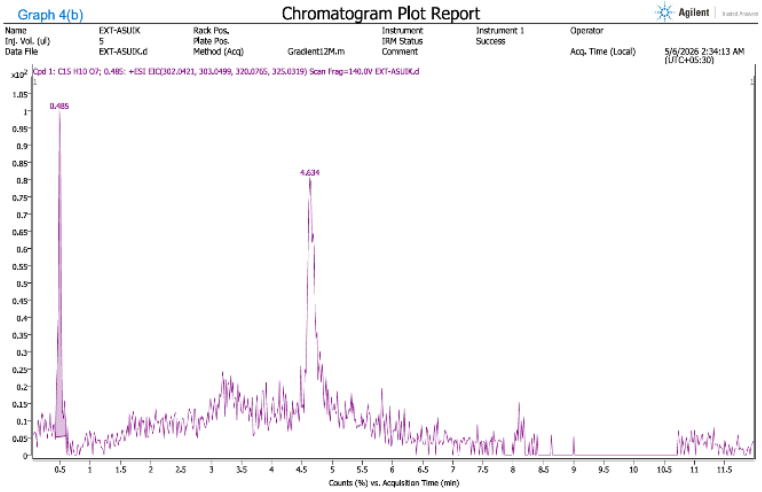

Figure 13 b: LC–MS chromatographic profile of the hydroethanolic extract of *Urginea indica* Kunth indicating the retention times of the detected $C_{15}H_{22}O$ compound.

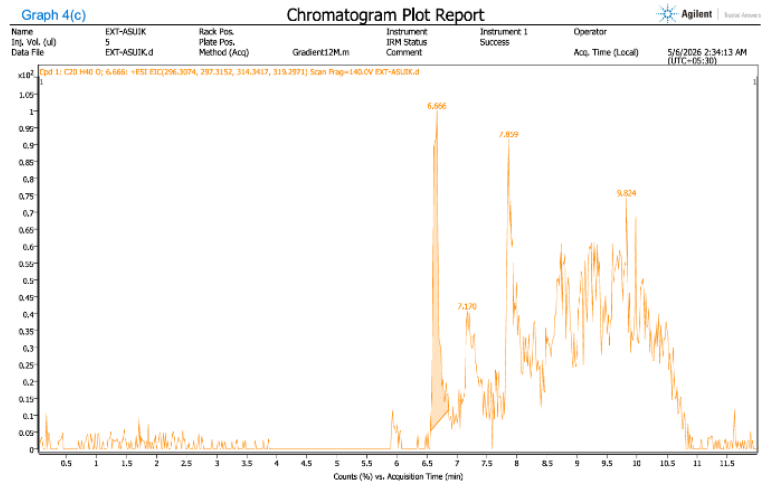

Figure 13 c: LC–MS chromatographic profile of the hydroethanolic extract of *Urginea indica* Kunth indicating the retention times of the detected $C_{20}H_{40}O$ compound.

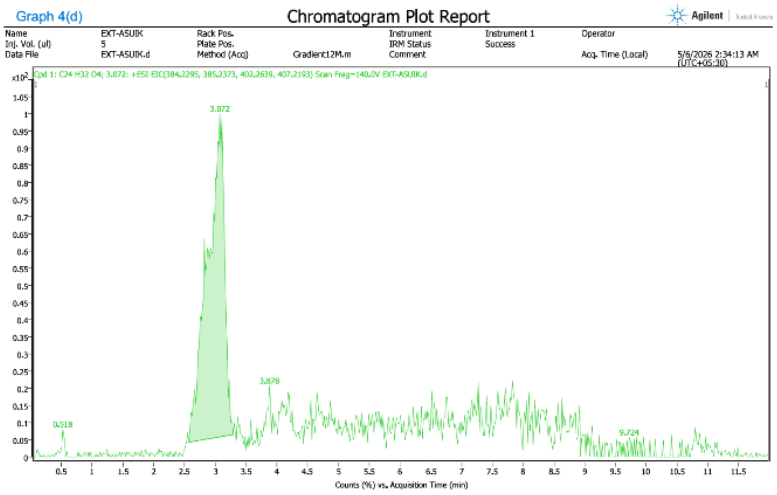

Figure 13 d: LC–MS chromatographic profile of the hydroethanolic extract of *Urginea indica* Kunth indicating the retention times of the detected $C_{14}H_{22}O$ compound.

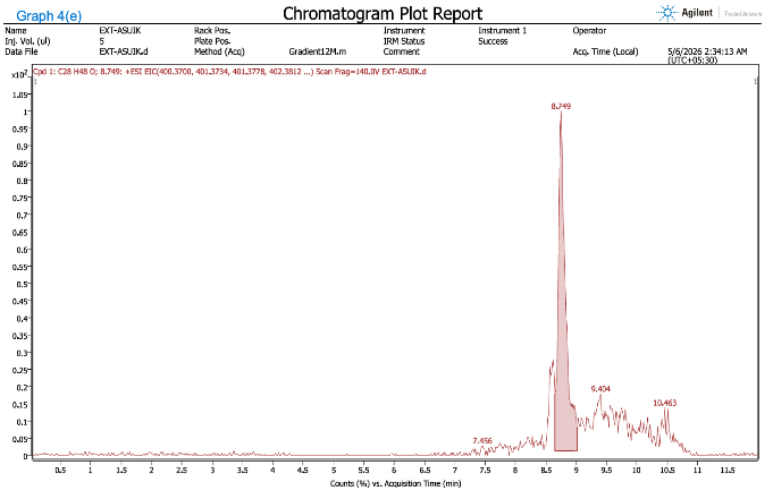

Figure 13 e: LC–MS chromatographic profile of the hydroethanolic extract of *Urginea indica* Kunth indicating the retention times of the detected $C_{14}H_{18}O$ compound.

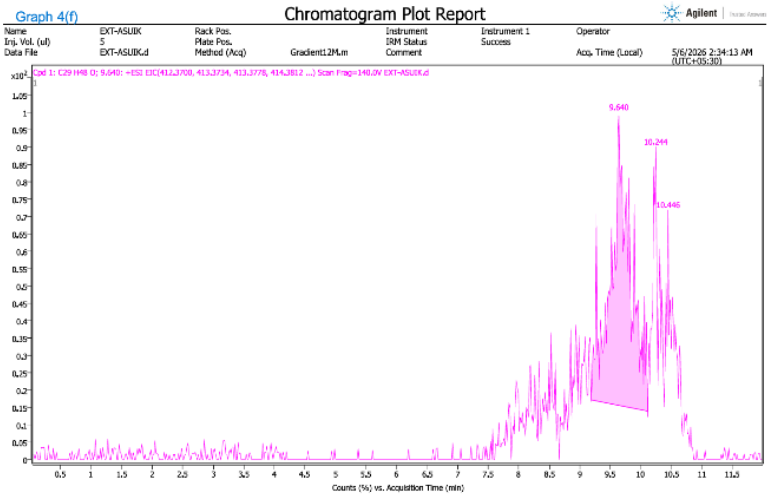

Figure 13 f: LC–MS chromatographic profile of the hydroethanolic extract of *Urginea indica* Kunth indicating the retention times of the detected compound.

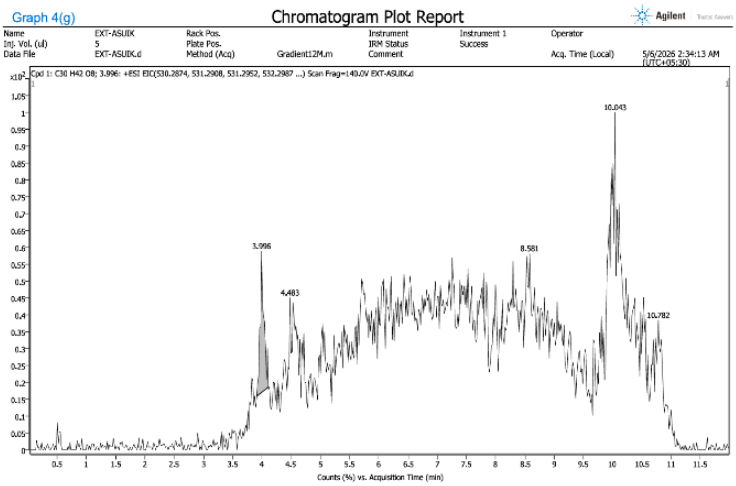

Figure 13 g: LC–MS chromatographic profile of the hydroethanolic extract of *Urginea indica* Kunth indicating the retention times of the detected compound.

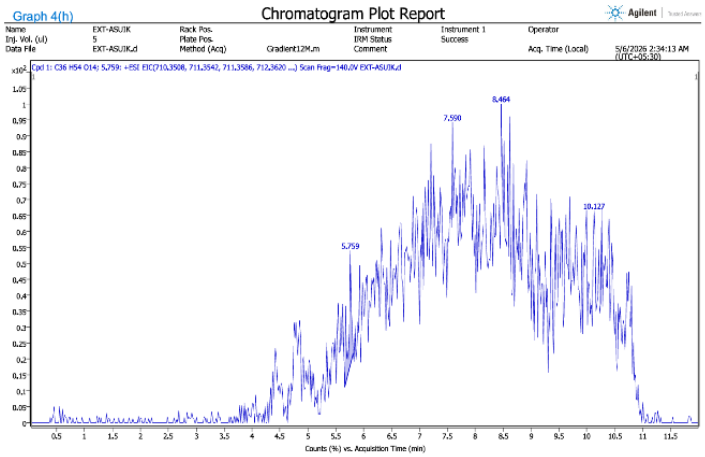

Figure 13 h: LC–MS chromatographic profile of the hydroethanolic extract of *Urginea indica* Kunth indicating the retention times of the detected compound.

Figure 13 (a-h): Overall graphical scheme for the green synthesis, structural characterization, morphological features, and LC–MS phytochemical profiling of zinc nanoparticles (ZnNPs) using Urginea indica Kunth extract.

The chromatogram corresponding to $C_{20}H_{40}O$ revealed several well-defined peaks distributed over the retention time range of 6.5–10.5 min, with the most intense peak at 6.666 min, followed by peaks at 7.170, 7.859, and 9.824 min, indicating multiple phytochemicals with similar molecular masses, while the broad chromatographic region between 8.0 and 10.5 min reflected the complex nature of the extract [Figure 13c]. The EIC corresponding to $C_{14}H_{22}O$ showed a sharp dominant peak at 3.272 min accompanied by a smaller peak at 3.978 min, suggesting the presence of a major constituent together with minor phytochemicals, with most compounds eluting during the early stage of chromatographic separation [Figure 13d]. The chromatogram of $C_{14}H_{18}O$ exhibited a prominent peak at 8.749 min and comparatively smaller peaks at 7.665, 9.404, and 10.463 min, indicating the predominance of one phytochemical along with several related constituents exhibiting moderate retention characteristics [Figure 13e]. The EIC corresponding to $C_{21}H_{32}O$ demonstrated a complex chromatographic profile, with low signal intensity during the initial stage followed by a gradual increase from approximately 7.5 min, producing prominent peaks at 9.449, 9.794, and 10.446 min, which suggested the presence of closely related phytochemicals or structural isomers with similar polarity and chromatographic behaviour [Figure 13f]. The chromatogram corresponding to $C_{18}H_{26}O$ displayed a broad cluster of overlapping peaks, beginning with a noticeable peak at 5.739 min, followed by several intense peaks between 6.5 and 9.5 min [Figure 13g], including the dominant peak at 8.494 min, while additional minor peaks extended up to 10.3 min, reflecting the rich phytochemical diversity of the hydroethanolic extract [Figure 13h]. The LC–MS chromatographic profiles confirm that the hydroethanolic extract of *Urginea indica* Kunth contains numerous phytochemical constituents with diverse chromatographic characteristics and molecular compositions. These metabolites are likely to contribute to the green synthesis of

zinc nanoparticles by acting as natural reducing and capping agents, facilitating zinc ion reduction and nanoparticle stabilisation [Figure 13]. Although the extracted ion chromatograms provide valuable information regarding retention behaviour and relative abundance, definitive identification of the detected compounds requires detailed interpretation of the corresponding mass spectra (m/z values), MS/MS fragmentation patterns, isotopic distributions, and comparison with authenticated reference standards or spectral databases.

5. CONCLUSION

This study successfully established an eco-friendly, green synthesis protocol for zinc nanoparticles (ZnNPs) using the hydroethanolic bulb extract of *Urginea indica* Kunth (Wild Onion) as a natural reducing, capping, and stabilizing agent. Comprehensive physicochemical characterization validated the bio-fabrication process [Figure 14]:

(i) Optical Confirmation: UV-Vis spectroscopy demonstrated a characteristic maximum absorption band at 288-290 nm absorbance, approx 0.76, confirming the formation of nanoscale zinc structures.

(ii) Crystallographic Profile: X-ray Diffraction (XRD) analysis confirmed the polycrystalline nature of the synthesized ZnNPs, with a primary diffraction peak at $2\theta = 32.5^0$ alongside minor crystalline phases (chlorite, quartz, and calcite) originating from plant-derived mineral matrices.

(iii) Morphological & Spatial Features: SEM and TEM imaging revealed predominantly quasi-spherical to irregular particles forming porous, densely packed aggregates. TEM line intensity profiling indicated nanoscale features around 0.28-0.30 nm in localized widths.

(iv) Elemental Composition & Purity: Energy-Dispersive X-ray Spectroscopy (EDX) confirmed zinc as the dominant element (77.3 wt%, 46.6 at %) with uniform spatial distribution demonstrated via EDS elemental mapping.

(v) Phytochemical Profiling: LC-MS/MS analysis identified a rich array of bioactive secondary metabolites in the *U. indica* extract (including compounds corresponding to $C_6H_6O_3$, $C_{15}H_{22}O$, $C_{20}H_{40}O$, $C_{14}H_{22}O$, $C_{14}H_{18}O$, and $C_{21}H_{32}O$, providing the redox-active functional groups necessary for Zn^{+2} reduction and surface passivation.

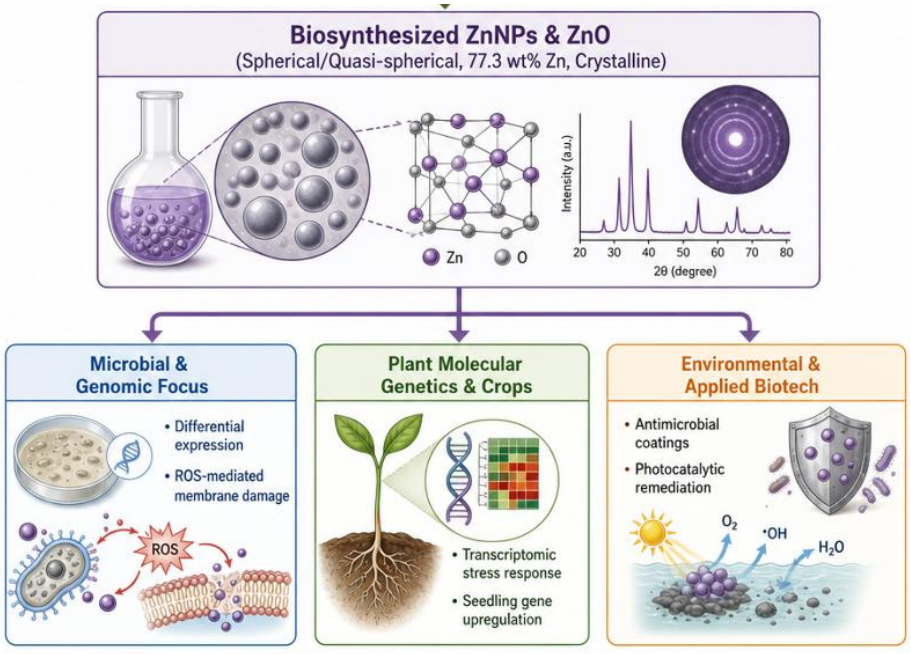

Figure 14. Schematic representation of biosynthesized ZnNPs & ZnO and their functional downstream applications.

While biogenic synthesis offers clear environmental advantages, several technical and analytical limitations remain to be addressed. Structurally, standard TEM resolution restricted measurements to localized lattice fringe spacings (0.28-0.30 nm) rather than full core diameters, omitting single-particle size distribution histograms and SAED patterns, while XRD revealed minor co-existing mineral phases (quartz, calcite) without quantitative Rietveld refinement. Phytochemically, high surface energy and biomolecular capping led to nanoparticle agglomeration rather than monodispersity, and LC-MS EICs lacked definitive MS/MS or NMR structural elucidation for specific capping molecules. The study remains limited to physicochemical characterization, lacking empirical *in vitro* or *in vivo* evaluations of cytotoxicity, biological safety, and specific genomic or transcriptomic responses.

Future research should focus on exploring the multidimensional applications and structural optimization of *U. indica*-synthesized ZnNPs through a integrated genomics, ecotoxicological, and bio-engineering framework. Key priorities include evaluating their genomic and mechanistic impact on multidrug-resistant microbes via RNA-Seq and ROS-mediated pathways, as well as assessing their potential as biostimulants in crops like *Oryza sativa* by tracking the upregulation of antioxidant (SOD, CAT, APX) and zinc-transporter (ZIP, ZNT) genes via RT-qPCR. Additionally, establishing biosafety, bioaccumulation, and cellular toxicity thresholds using model organisms (*A. thaliana*, *C. elegans*, *D. rerio*) will be essential before field application. Particle synthesis should be refined using Response Surface Methodology (RSM) alongside advanced analytical techniques—such as HRTEM, SAED, XPS, and FTIR—to minimize agglomeration, ensure monodispersity, and precisely define surface ligand dynamics [Figure 15].

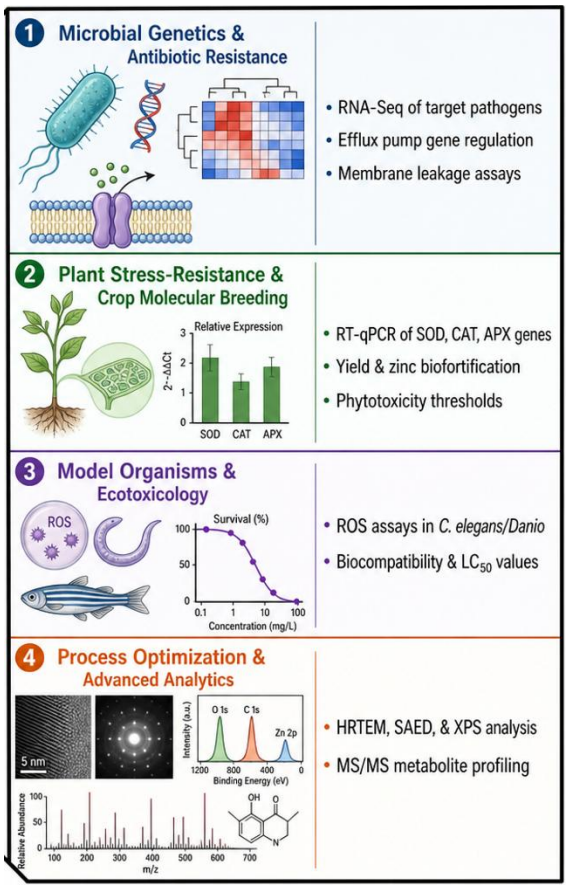

Figure 15. Strategic Future Research Roadmap Categorized into Key Experimental Domains.

Conflict of Interest

The authors declare that there are no conflicts of interest regarding the publication of this research.

Funding

The authors received no specific financial support from any funding agency in the public, commercial or not-for-profit sectors for the conduct of this research.

Ethical Considerations

The study was conducted in accordance with accepted ethical standards. Participation was entirely voluntary, and informed consent was obtained from all participants before data collection. Participant confidentiality and anonymity were strictly maintained throughout the study, and the collected data were used exclusively for academic and research purposes

REFERENCES:

1. Aggarwal, J., & Alam, T. (2020). Green synthesis of zinc oxide nanoparticles and their antibacterial properties using plant extract of *Aristolochia elegans*. *Asian Journal of Chemistry, 32*(10), 2589–2593. https://doi.org/10.14233/ajchem.2020.22812
2. Ahmad, H., Venugopal, K., Rajagopal, K., De Britto, S., Nandini, B., Pushpalatha, H. G., ... & Jogaiah, S. (2020). Green synthesis and characterization of zinc oxide nanoparticles using Eucalyptus globules and

their fungicidal ability against pathogenic fungi of apple orchards. *Biomolecules*, *10*(3), 425. https://doi.org/10.3390/biom10030425

3. Ahmed, S., Ahmad, M., Swami, B. L., & Ikram, S. (2016). A review on plants extract mediated synthesis of silver nanoparticles for antimicrobial applications: a green expertise. *Journal of advanced research*, *7*(1), 17-28. https://doi.org/10.1016/j.jare.2015.02.007
4. Ahmed, S., Annu, Chaudhry, S. A., & Ikram, S. (2017). A review on biogenic synthesis of ZnO nanoparticles using plant extracts and microbes: A prospect towards green chemistry. *Journal of Photochemistry and Photobiology B: Biology, 166*, 272–284. https://doi.org/10.1016/j.jphotobiol.2016.12.011
5. Ajayan, A. S., & Hebsur, N. S. (2020). Green synthesis of zinc oxide nanoparticles using neem (*Azadirachta indica*) and tulasi (*Ocimum tenuiflorum*) leaf extract and their characterization. *International Journal of Current Microbiology and Applied Sciences, 9*(2), 277–285. https://doi.org/10.20546/ijcmas.2020.902.035
6. Akbar Jan, F., Ullah, R., Ullah, N., & Usman, M. (2021). Exploring the environmental and potential therapeutic applications of Myrtus communis L. assisted synthesized zinc oxide (ZnO) and iron doped zinc oxide (Fe-ZnO) nanoparticles. *Journal of Saudi Chemical Society*, *25*(7), 101278. https://doi.org/10.1016/j.jscs.2021.101278
7. Akhtar, M. S., Panwar, J., & Yun, Y.-S. (2013). Biogenic synthesis of metallic nanoparticles by plant extracts. *ACS Sustainable Chemistry & Engineering, 1*(6), 591–602. https://doi.org/10.1021/sc300118u
8. Alarfaj, N. A., Alshehri, E. M., Al-Tamimi, S. A., & El-Tohamy, M. F. (2024). Plant extract mediated synthesis of ZnO and CeO_2 nanoparticles for spectrofluorometric assay of omeprazole and domperidone in pharmaceuticals. *Heliyon, 10*(4), e26164. https://doi.org/10.1016/j.heliyon.2024.e26164
9. Al-Darwesh, M. Y., Ibrahim, S. S., & Mohammed, M. A. (2024). A review on plant extract mediated green synthesis of zinc oxide nanoparticles and their biomedical applications. *Results in Chemistry, 7*, 101368. https://doi.org/10.1016/j.rechem.2024.101368
10. Anand, S., Choubey, S., Vaishnav, S., Sharma, V., & Shahi, S. (2026) Biogenic Zinc Nanoparticles Derived from Curcuma longa and Zingiber officinale: A Comparative Study. Journal for Research in *Applied Sciences and Biotechnology*, 5(1), 188–198. https://doi.org/10.55544/jrasb.5.1.24
11. Arya, K. Y., Shahi, S. (2025) Citrus-Mediated Green Synthesis of Zinc Nanoparticles: A Comparative Study. *International Journal of Environmental Sciences*, 11(4s), 778-790, https://theaspd.com/index.php/ijes/article/view/628
12. Aswal, S., Kumar, A., Semwal, R. B., Chauhan, A., Kumar, A., Lehmann, J., & Semwal, D. K. (2019). *Drimia indica*: A plant used in traditional medicine and its potential for clinical uses. *Medicina, 55*(6), 255. https://doi.org/10.3390/medicina55060255
13. Awasthi S, Shahi S. (2026) Berry Bliss: A Comparative Study of the Zinc Nanoparticles Synthesized from Gooseberry, Strawberry, Blueberry, and Cranberry Extracts. *International Journal Drug Delivery Technology*. 16(18s), 550-557. https://doi.org/10.25258/ijddt.16.18s.59
14. Bhalla, N., Ingle, N., Jayaprakash, A., Patel, H., Patri, S. V., & Haranath, D. (2023). Green approach to synthesize nano zinc oxide via Moringa oleifera leaves for enhanced anti-oxidant, anti-acne and anti-bacterial properties for health & wellness applications. *Arabian Journal of Chemistry*, *16*(1), 104506. https://doi.org/10.1016/j.arabjc.2022.104506
15. Chormey, D. S., Zaman, B. T., Borahan Kustanto, T., Erarpat Bodur, S., Bodur, S., Tekin, Z., Nejati, O., & Bakırdere, S. (2023). Biogenic synthesis of novel nanomaterials and their applications. *Nanoscale, 15*, 19423–19447. https://doi.org/10.1039/d3nr03843b
16. Dash, P., Gochhi, M., & Ghosh, G. (2023). Green synthesis of zinc oxide nanoparticles using the plant extract of Myristica fragrans and their antibacterial activity assessment. *Minerva Biotechnology & Biomolecular Research*, *35*(2), 81. https://doi.org/10.23736/S2724-542X.23.02957-7
17. Degefa, A., Bekele, B., Jule, L. T., Fikadu, B., Ramaswamy, S., Dwarampudi, L. P., ... & Ramaswamy, K. (2021). Green Synthesis, Characterization of Zinc Oxide Nanoparticles, and Examination of Properties for Dye-Sensitive Solar Cells Using Various Vegetable Extracts. *Journal of Nanomaterials*, *2021*(1), 3941923. https://doi.org/10.1155/2021/3941923Digital
18. Dhatwalia, B., & Sharma, N. (2024). Phytochemical analysis of phenolic compounds by using LCMS of Urginea indica. *Journal of Ayurveda and Holistic Medicine (JAHM)*, *12*(5). https://doi.org/10.70066/jahm.v12i5.1374
19. El-Seedi, H. R., El-Shabasy, R. M., Khalifa, S. A. M., Saeed, A., Shah, A., Shah, R., Iftikhar, F. J., Abdel-Daim, M. M., Omri, A., Hajrah, N. H., Sabir, J. S. M., Zou, X., Halabi, M. F., Sarhan, W., & Guo, W. (2019). Metal nanoparticles fabricated by green chemistry using natural extracts: Biosynthesis, mechanisms, and applications. *RSC Advances, 9*, 24539–24559. https://doi.org/10.1039/c9ra02225b
20. Elumalai, K., & Velmurugan, S. (2015). Green synthesis, characterization and antimicrobial activities of zinc oxide nanoparticles from the leaf extract of Azadirachta indica (L.). *Applied Surface Science*, *345*, 329-336. https://doi.org/10.1016/j.apsusc.2015.03.176

21. Fakhari, S., Jamzad, M., & Kabiri Fard, H. (2019). Green synthesis of zinc oxide nanoparticles: a comparison. *Green chemistry letters and reviews*, *12*(1), 19-24. https://doi.org/10.1080/17518253.2018.1547925
22. Gunalan, S., Sivaraj, R., & Rajendran, V. (2012). Green synthesized ZnO nanoparticles against bacterial and fungal pathogens. *Progress in Natural Science: Materials International*, *22*(6), 693-700. https://doi.org/10.1016/j.pnsc.2012.11.015
23. Hamed, R., Obeid, R. Z., & Abu-Huwaij, R. (2023). Plant mediated-green synthesis of zinc oxide nanoparticles: An insight into biomedical applications. *Nanotechnology Reviews, 12*(1), 20230112. https://doi.org/10.1515/ntrev-2023-0112
24. Iravani, S. (2011). Green synthesis of metal nanoparticles using plants. *Green Chemistry, 13*(10), 2638–2650. https://doi.org/10.1039/c1gc15386b
25. Islam, M. F., Islam, S., Miah, M. A. S., Huq, A. K. O., Saha, A. K., Mou, Z. J., Mondol, M. M. H., & Bhuiyan, M. N. I. (2024). Green synthesis of zinc oxide nanoparticles using *Allium cepa* L. waste peel extracts and its antioxidant and antibacterial activities. *Heliyon, 10*(3), e25430. DOI: https://doi.org/10.1016/j.heliyon.2024.e25430
26. Iswarya, M., Sudha, P., Kalaiselvi, V., Ramya, V., & Shanmathi, S. (2020). *Solanum nigrum* leaf extract capped synthesis of ZnO nanoparticles. *Journal of Environmental Nanotechnology, 9*(4), 37–41. https://doi.org/10.13074/jent.2020.12.204424
27. John, D. M., Pillai, N. S., Sivan, A., P., L., P., A., Sreekanth, K. M., Sivasubramanian, G., & Sreedhar, K. M. (2024). Ferromagnetic ZnO nanostructures from an organo zinc complex formulated via *Piper longum* L.-assisted green synthesis: Multifaceted prospects in photocatalysis, antimicrobial activity, and cell viability studies. *Heliyon, 10*(13), e33360. https://doi.org/10.1016/j.heliyon.2024.e33360
28. Kumar, A., Shrivastava, A., Suttee, A., Gupta, P., Shahi, S., Barik, R., Chaturvedi, P., & Dwivedi, S. (2026) Plant-Powered Nanotechnology: A Review of Green Synthesis Approaches for ZnO and Silver Nanoparticles with Medicinal Flora. *Current Topics in Medicinal Chemistry*, 28, https://doi.org/10.2174/0115680266413831251120132852
29. Kumar, M. N., Rahale, C. S., Shanmugam, H., Vanitha, K., Saranya, N., & Prasanthrajan, M. (2023). Eco-friendly Synthesis of Zinc Oxide Nanoparticles Using Camellia sinensis (Green Tea) and Its Characterization. *International Journal of Plant & Soil Science*, *35*(20), 56-61. https://doi.org/10.9734/ijpss/2023/v35i203785.
30. Maheswaran, H., Djearamane, S., Dhanapal, A. C. T. A., & Wong, L. S. (2024). Cytotoxicity of green synthesized zinc oxide nanoparticles using *Musa acuminata* on Vero cells. *Heliyon, 10*(11), e31316. DOI: https://doi.org/10.1016/j.heliyon.2024.e31316
31. Michen, B., Geers, C., Vanhecke, D., Endes, C., Rothen-Rutishauser, B., Balog, S., & Petri-Fink, A. (2015). Avoiding drying-artifacts in transmission electron microscopy: Characterizing the size and colloidal state of nanoparticles. *Scientific reports*, *5*(1), 9793. https://doi.org/10.1038/srep09793
32. Muniz, F. T. L., Miranda, M. R., Morilla dos Santos, C., & Sasaki, J. M. (2016). The Scherrer equation and the dynamical theory of X-ray diffraction. *Foundations of Crystallography*, *72*(3), 385-390. https://doi.org/10.1107/S205327331600365X
33. Nava, O. J., Luque, P. A., Gómez-Gutiérrez, C. M., Vilchis-Nestor, A. R., Castro-Beltrán, A., Mota-González, M. L., & Olivas, A. (2017). Influence of Camellia sinensis extract on Zinc Oxide nanoparticle green synthesis. *Journal of Molecular Structure*, *1134*, 121-125. https://doi.org/10.1016/j.molstruc.2016.12.069
34. Pandey, S., Shahi, S. (2025) Pterocarpus marsupium as a "Green Nanofactory": A Comparative Review of Biosynthesized Gold, Silver, Copper, and Zinc Nanoparticles for Therapeutic Applications. *NeuroQuantology*, 23(8), 348-357, https://doi.org/10.48047/nq.2025.23.8.nq25030
35. Patterson, A. L. (1939). The Scherrer formula for X-ray particle size determination. *Physical Review, 56*(10), 978–982. https://doi.org/10.1103/PhysRev.56.978
36. Peta, S., & Singh, S. (2025). Green synthesis of zinc oxide nanoparticles using plant extract for catalysis applications. *Nanoscale, 17*, 3708–3713. https://doi.org/10.1039/d4nr03581j
37. Rajabi, H. R., Naghiha, R., Kheirizadeh, M., Sadatfaraji, H., Mirzaei, A., & Alvand, Z. M. (2017). Microwave assisted extraction as an efficient approach for biosynthesis of zinc oxide nanoparticles: synthesis, characterization, and biological properties. *Materials Science and Engineering: C*, *78*, 1109-1118.https://doi.org/10.1016/j.msec.2017.03.090
38. Raveendran, P., Fu, J., & Wallen, S. L. (2003). Completely “green” synthesis and stabilization of metal nanoparticles. *Journal of the American Chemical Society, 125*(46), 13940–13941. https://doi.org/10.1021/ja029267j
39. Şahin, B., Soylu, S. O. N. E. R., Kara, M. E. R. V. E., Türkmen, M. U. S. A., Aydin, R., & Çetin, H. İ. D. A. Y. E. T. (2021). Superior antibacterial activity against seed-borne plant bacterial disease agents and enhanced physical properties of novel green synthesized nanostructured ZnO using Thymbra spicata plant extract. *Ceramics International*, *47*(1), 341-350.https://doi.org/10.1016/j.ceramint.2020.08.139

40. Samat, N. A., & Nor, R. M. (2013). Sol–gel synthesis of zinc oxide nanoparticles using Citrus aurantifolia extracts. *Ceramics International*, *39*, S545-S548. https://doi.org/10.1016/j.ceramint.2012.10.132
41. Sangeetha, G., Rajeshwari, S., & Venckatesh, R. (2011). Green synthesis of zinc oxide nanoparticles by aloe barbadensis miller leaf extract: Structure and optical properties. *Materials Research Bulletin*, *46*(12), 2560-2566. https://doi.org/10.1016/j.materresbull.2011.07.046
42. Sedefoglu, N. (2024). Green synthesis of ZnO nanoparticles by Myrtus communis plant extract with investigation of effect of precursor, calcination temperature and study of photocatalytic performance. *Ceramics International*, *50*(6), 9884-9895. https://doi.org/10.1016/j.ceramint.2024.01.387
43. Selim, Y. A., Azb, M. A., Ragab, I., & HM Abd El-Azim, M. (2020). Green synthesis of zinc oxide nanoparticles using aqueous extract of Deverra tortuosa and their cytotoxic activities. *Scientific reports*, *10*(1), 3445. https://doi.org/10.1038/s41598-020-60541-1
44. Shahi, S. (2025) Tailoring Metal Nanoparticles: A Comparative Assessment of Au, Ag, Cu, Zn, Pt, and Fe for Targeted Applications. *Stallion Journal for Multidisciplinary Associated Research Studies*, 4 (2), 320–331. https://doi.org/10.55544/sjmars.4.2.22
45. Sharma, D., Kanchi, S., & Bisetty, K. (2019). Biogenic synthesis of nanoparticles: A review. *Arabian Journal of Chemistry, 12*(8), 3576–3600. https://doi.org/10.1016/j.arabjc.2015.11.002
46. Singh, H., Desimone, M. F., Pandya, S., Jasani, S., George, N., Adnan, M., ... & Alderhami, S. A. (2023). Revisiting the green synthesis of nanoparticles: uncovering influences of plant extracts as reducing agents for enhanced synthesis efficiency and its biomedical applications. *International journal of nanomedicine*, 4727-4750. https://doi.org/10.2147/IJN.S419369
47. Suresh, D., Shobharani, R. M., Nethravathi, P. C., Kumar, M. P., Nagabhushana, H., & Sharma, S. C. (2015). Artocarpus gomezianus aided green synthesis of ZnO nanoparticles: Luminescence, photocatalytic and antioxidant properties. *Spectrochimica Acta Part A: Molecular and Biomolecular Spectroscopy*, *141*, 128-134. https://doi.org/10.1016/j.saa.2015.01.048
48. Swetharanyam, A., Kunjitham, R., & Barnwal, J. (2020). Plant mediated synthesis of zinc oxide nanoparticles and their potential applications as photocatalyst and antibacterial agents. *Asian Journal of Chemistry, 32*(11). https://doi.org/10.14233/ajchem.2020.22971
49. Thakur, S., Shandilya, M., & Guleria, G. (2021). Appraisement of antimicrobial zinc oxide nanoparticles through Cannabis Jatropha curcasa Alovera and Tinosporacordifolia leaves by green synthesis process. *Journal of Environmental Chemical Engineering*, *9*(1), 104882. https://doi.org/10.1016/j.jece.2020.104882
50. Tripathy, P., Shahi, S. (2025) Biogenic Zinc Oxide Nanoparticles from *Agaricus bisporus* for Advanced Glycoconjugate Recognition and Biomedical Sensing. *Journal for Research in Applied Sciences and Biotechnology*, 4(5), 114-122. https://doi.org/10.55544/jrasb.4.5.12
51. Ukidave, V. V., & Ingale, L. T. (2022). Green synthesis of zinc oxide nanoparticles from coriandrum sativum and their use as fertilizer on Bengal gram, Turkish gram, and green gram plant growth. *International Journal of Agronomy*, *2022*(1), 8310038. https://doi.org/10.1155/2022/8310038
52. Verma, R., Pathak, S., Srivastava, A. K., Prawer, S., & Tomljenovic-Hanic, S. (2021). ZnO nanomaterials: Green synthesis, toxicity evaluation and new insights in biomedical applications. *Journal of Alloys and Compounds, 876*, 160175. https://doi.org/10.1016/j.jallcom.2021.160175
53. Vijayakumar, S., Vaseeharan, B., Malaikozhundan, B., & Shobiya, M. (2016). Laurus nobilis leaf extract mediated green synthesis of ZnO nanoparticles: Characterization and biomedical applications. *Biomedicine & Pharmacotherapy*, *84*, 1213-1222. https://doi.org/10.1016/j.biopha.2016.10.038
54. Xu, J., Huang, Y., Zhu, S., Abbes, N., Jing, X., & Zhang, L. (2021). A review of the green synthesis of ZnO nanoparticles using plant extracts and their prospects for application in antibacterial textiles. *Journal of Engineered Fibers and Fabrics, 16*. https://doi.org/10.1177/15589250211046242
55. Yadi, M., Mostafavi, E., Saleh, B., Davaran, S., Aliyeva, I., Khalilov, R., ... & Milani, M. (2018). Current developments in green synthesis of metallic nanoparticles using plant extracts: a review. *Artificial cells, nanomedicine, and biotechnology*, *46*(sup3), 336-343. https://doi.org/10.1080/21691401.2018.1492931
56. Yuvakkumar, R., Suresh, J., Nathanael, A. J., Sundrarajan, M., & Hong, S. I. (2014). Novel green synthetic strategy to prepare ZnO nanocrystals using rambutan (Nephelium lappaceum L.) peel extract and its antibacterial applications. *Materials Science and Engineering: C*, *41*, 17-27. https://doi.org/10.1016/j.msec.2014.04.025